

Changes in m6A RNA methylation contribute to heart failure progression by modulating translation

Tea Berulava^{1†}, Eric Buchholz^{2,7†}, Vakhtang Elerdashvili^{1,3}, Tonatiuh Pena^{1,3}, Md Rezaul Islam¹, Dawid Lbik^{2,7}, Belal A. Mohamed^{2,7}, Andre Renner⁴, Dirk von Lewinski⁵, Michael Sacherer⁵, Katherine E. Bohnsack⁶, Markus T. Bohnsack⁶, Gaurav Jain^{1,3}, Vincenzo Capece¹, Nicole Cleve¹, Susanne Burkhardt¹, Gerd Hasenfuss^{2,7}, Andre Fischer^{1,8,9*‡}, and Karl Toischer^{2,7*‡}

¹Department for Epigenetics and Systems Medicine in Neurodegenerative Diseases, German Center for Neurodegenerative Diseases (DZNE), Göttingen, Germany; ²Clinic for Cardiology and Pneumology, University Medical Center, Göttingen, Germany; ³Bioinformatics Unit, German Center for Neurodegenerative Diseases (DZNE), Göttingen, Germany; ⁴Clinic for Thoracic and Cardiovascular Surgery, Heart and Diabetes Centre NRW, Ruhr-University Bochum, Bochum, Germany; ⁵Department of Cardiology, Medical University Graz, Graz, Austria; ⁶Department of Molecular Biology, University Medical Center, Göttingen, Germany; ⁷German Centre for Cardiovascular Research (DZHK), partner site Göttingen, Göttingen, Germany; ⁸Department of Psychiatry and Psychotherapy, University Medical Center, Göttingen, Germany; and ⁹Cluster of Excellence "Multiscale Bioimaging: from Molecular Machines to Networks of Excitable Cells" (MBExC), University of Göttingen, Germany

Received 28 June 2019; revised 15 September 2019; accepted 15 October 2019; online publish-ahead-of-print 17 December 2019

Aims

Deregulation of epigenetic processes and aberrant gene expression are important mechanisms in heart failure. Here we studied the potential relevance of m6A RNA methylation in heart failure development.

Methods and results

We analysed m6A RNA methylation via next-generation sequencing. We found that approximately one quarter of the transcripts in the healthy mouse and human heart exhibit m6A RNA methylation. During progression to heart failure we observed that changes in m6A RNA methylation exceed changes in gene expression both in mouse and human. RNAs with altered m6A RNA methylation were mainly linked to metabolic and regulatory pathways, while changes in RNA expression level mainly represented changes in structural plasticity. Mechanistically, we could link m6A RNA methylation to altered RNA translation and protein production. Interestingly, differentially methylated but not differentially expressed RNAs showed differential polysomal occupancy, indicating transcription-independent modulation of translation. Furthermore, mice with a cardiomyocyte restricted knockout of the RNA demethylase Fto exhibited an impaired cardiac function compared to control mice.

Conclusions

We could show that m6A landscape is altered in heart hypertrophy and heart failure. m6A RNA methylation changes lead to changes in protein abundance, unconnected to mRNA levels. This uncovers a new transcription-independent mechanisms of translation regulation. Therefore, our data suggest that modulation of epitranscriptomic processes such as m6A methylation might be an interesting target for therapeutic interventions.

Keywords

Heart failure • RNA methylation • Epitranscriptomics • Translation

*Corresponding authors. Karl Toischer, Department of Cardiology and Pneumology, Georg-August-University, Universität Göttingen, Robert-Koch-Str. 40, 37075 Göttingen, Germany. Tel: +49 551 3966318, Fax: +49 551 3922953, Email: ktoischer@med.uni-goettingen.de
 Andre Fischer, Department for Epigenetics and Systems Medicine, German Center for Neurodegenerative diseases, von Siebold Str. 3A, 37075 Göttingen, Germany Tel: +49 551 3961211, Fax: +49 551 3961214, Email: andre.fischer@dzne.de

[†]These authors contributed equally as first authors.

[‡]These authors contributed equally as senior authors.

Introduction

Heart failure, characterized by reduced cardiac function and left ventricular dilatation, is a leading cause of hospital admission and mortality.¹ This process is accompanied by increased apoptosis, fibrosis and changes in gene expression.^{2,3} Until now, inhibition of neuroendocrine stimulation is the only treatment for heart failure; however, the therapeutic efficacy of this approach is limited and cannot prevent the eventual progression of the disease.⁴ Therefore, additional therapeutic options are needed.

There is increasing evidence that aberrant gene expression, orchestrated by transcription factors and epigenetic processes such as non-coding RNAs, DNA and histone modifications, represents a key event in heart failure and could thus offer new ways for therapeutic intervention.^{5,6} While methylation of DNA seems to be important during maturation of the heart,⁷ the role of RNA modifications has not been studied in detail until now.

N6-adenosine methylation (m6A) of RNA transcripts is the most prevalent modification found in many classes of RNA.⁸ Similar to epigenetic changes in DNA and histone modifications, m6A in RNA is dynamic and reversible.^{8–10} In all classes of RNA, m6A mainly occurs within a highly-conserved consensus motif identified as RRACH (R=G or A, H=A, C or U). The formation of m6A is regulated by methyltransferases (METTL3, METTL14, WTAP, METTL16)^{11,12} and demethylases (FTO, ALKBH5).^{13,14} m6A recognizing proteins such as members of the YTH domain protein family and HNRNPA2B1 are involved in processes regulating the fate of target transcripts. The current data suggest that the degree and the pattern of methylation of mRNAs can affect their splicing, transport, storage, translation and/or decay.¹⁰

At present, there is only one recent study which reported a role for m6A in the peri-infarct zone after myocardial infarction.¹⁵ In our study, we consequently applied transcriptome-wide approaches and defined changes in m6A in mouse and human heart failure development. We found that m6A RNA methylation appears to affect cardiac signalling and metabolic processes by modulation of translation. Our data provide evidence that m6A RNA methylation is involved in heart failure development and might be a novel therapeutic target.

Methods

See online supplementary *Methods S1* for detailed description. The investigation conforms to the principles outlined in the Declaration of Helsinki and the Guide for the Care and Use of Laboratory Animals (NIH publication No. 85–23, revised 1996). All patients provided written informed consent for the use of cardiac tissue samples. Surgery on mice was done using a minimally invasive approach. Echocardiography was performed on anaesthetized animals.

RNA isolation from left ventricles was performed with Trizol reagent according to the manufacturer's instruction. DNase treated and fragmented RNA was subjected first to immunoprecipitation with anti-m6A antibody (Synaptic Systems, #202003) and then to high-throughput sequencing on Illumina 2000 platform. Generated reads were mapped to mm10 and hg19, and peaks showing significant enrichment for m6A in immunoprecipitated samples compared to corresponding input samples were detected with the MeTPeak

package.¹⁶ For the polysomal occupancy experiment, RNA extracted from polysomal fractions of the snap-frozen tissues was sequenced on the Illumina HiSeq2000. Differential methylation analysis was done using an in-house developed pipeline. Deseq2 was used for differential gene expression and differential polysome binding analysis. mRNAs showing significant (Padj < 0.05) and at least two-fold change in m6A levels, mRNA levels and polysome binding are reported in this study. Differential m6A methylation was further verified using qRT-PCR on RNAs immunoprecipitated with anti-m6A antibody without fragmentation. Western blot analysis for different protein level evaluation was performed following manufacturer's instructions for the corresponding antibodies. We used the ClueGo plug-in in the Cytoscape software for pathway analysis for genes identified in different experiments.

Results

m6A RNA methylation in the adult heart

Fto, Mettl3 and Mettl14 as the key regulators of m6A RNA methylation are expressed in the adult mouse heart (Figure 1A and online supplementary Figure S9). Transcriptome-wide analysis of m6A RNA methylation via m6A-specific methylated RNA immunoprecipitation followed by next-generation sequencing (MeRIP-Seq)¹⁷ revealed that 24% of all detected transcripts carry m6A marks ($n = 5$). More specifically, we detected 3208 peaks linked to 2164 transcripts (Figure 1B and online supplementary Table S4). The quality of our data was confirmed by an unbiased motif search using the detected m6A peaks as input that identified the previously reported m6A consensus sequence RRACH (Figure 1C). Relative quantification of m6A peaks across all transcripts showed a distribution similar as in other tissues^{17–19} with an enrichment of m6A toward the translation end site (Figure 1D).

The majority of the m6A-containing transcripts carried this mark in the 5'UTR or 3'UTR and the coding sequence (CDS). Only a negligible number of transcripts were exclusively m6A-methylated in 5'UTR ($n = 9$) or 3'UTR ($n = 163$) (Figure 1E). A gene ontology (GO) analysis revealed that transcripts with m6A in the 5'UTR and/or CDS were linked to energy metabolism, mitochondrial function and intra-cellular signalling, while transcripts methylated in the 3'UTR mostly code for proteins involved in pathways linked to more specific metabolic processes such as 'acetyl-CoA or glycerol biosynthesis' and 'positive regulation of protein dephosphorylation' (Figure 1F).

Transcripts that carry m6A in the 5'UTR and CDS showed a mild positive correlation of m6A marks with expression level ($r = 0.10$, $P = 5.86 \times 10^{-7}$; Figure 1G), whereas methylation marks within the 3'UTR showed a mild negative correlation ($r = -0.08$, $P = 0.006$; Figure 1G). We also detected long non-coding RNAs with m6A marks (online supplementary Figure S1A), but here m6A was not correlated to its expression level ($r = 0.06$, $P = 0.72$; online supplementary Figure S1B). A detailed annotation of the m6A-containing non-coding peaks is found in online supplementary Table S4.

Cardiac hypertrophy and failure are linked to substantial changes in m6A

Next, we studied m6A RNA methylation during the progression of heart failure. Therefore we used the mouse model of

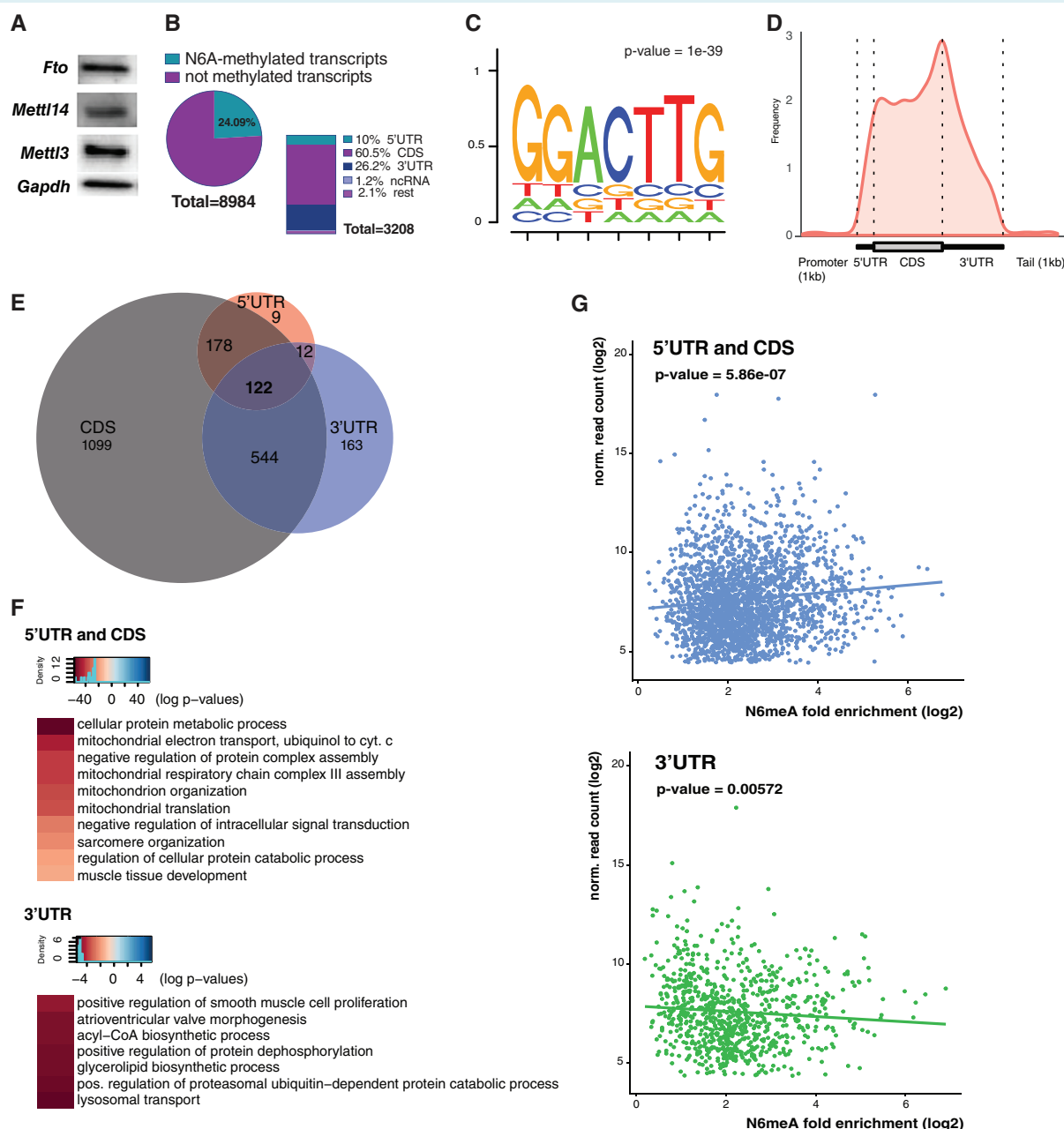
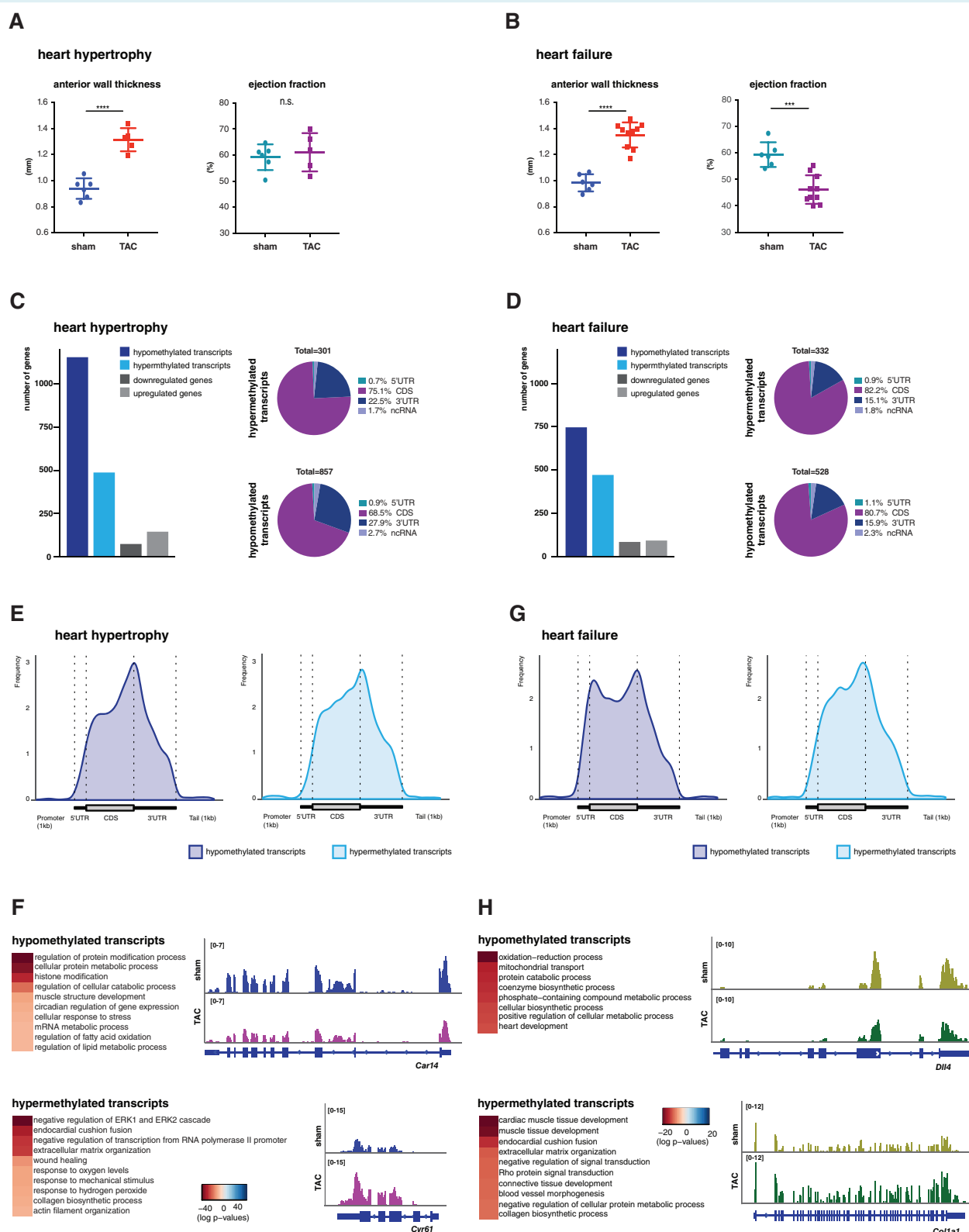


Figure 1 m6A RNA methylation in the healthy mouse heart. (A) Representative western blot images showing expression of Fto, Mettl3 and Mettl14 protein in mouse heart tissue. (B) Pie and bar charts showing the amount and distribution of m6A RNA methylation in the mouse heart. (C) Sequence motif identified within m6A peaks. (D) Distribution of m6A peaks across mRNA transcripts. (E) Venn diagram showing methylation marks across transcript regions. (F) Heat map showing pathway analysis of transcripts that carry m6A marks in either 5'UTR and CDS or 3'UTR. (G) Correlation analysis between transcript level and m6A methylation at 5'UTR and CDS (upper panel) and 3'UTR (lower panel). $n = 5$ per group.

transverse aortic constriction (TAC) to induce pressure overload.³ One week after TAC mice responded with compensated hypertrophy (Figure 2A), whereas after 8 weeks heart failure developed (Figure 2B). In addition to m6A RNA methylation, we also analysed expression changes from the same material by RNA Seq.

We detected a number of differentially expressed genes either 1 or 8 weeks after TAC that were mainly linked to structural cardiac plasticity pathways ($n = 6$ per group; online supplementary Figure S2, Tables S3 and S4). Using the same cut-offs as for the detection of differential methylated transcripts ($\text{Log2FC} > 1$, $\text{Padj} < 0.05$) we observed that at both time points after TAC



the number of transcripts with significant changes in m6A was much higher than the number of differentially expressed genes [Figure 2C and 2D; 1 week: 1638 transcripts differentially methylated, 217 differentially expressed (online supplementary Figure S2 and Table S3); 8 weeks: 1215 transcripts differentially methylated and 174 differentially expressed (online supplementary Figure S2 and Table S4)]. The global distribution of m6A marks across hyper- and hypomethylation 1 week after TAC did not differ from control (Figure 2E and 2G), whereas in case of 8 weeks after TAC a significant shift toward hypomethylation specifically at the transcription start site (TSS) was visible with an area under the curve (AUC) of 0.2733 (95% confidence interval 0.2731–0.2735) for hypomethylation whereas AUC for hypermethylation at 5'UTR was 0.1617 (95% confidence interval 0.1614–0.1619) (Figure 2G). Transcripts affected by m6A RNA methylation were substantially different from the transcripts affected at the level of expression (online supplementary Figure S3, Tables S3 and S4), suggesting that changes in m6A RNA methylation and the regulation of transcript level likely represent distinct cellular processes.

Next, we performed a GO analysis of differentially methylated transcripts. Interestingly, only few pathways involved in contractile or structural processes could be detected. However, both hypo- and hypermethylated transcripts in case of heart hypertrophy were enriched in GO categories linked to metabolic processes and gene expression regulation such as 'histone modification' and 'cellular response to stress' (Figure 2F). Additionally, hypermethylated transcripts were linked to signalling pathways such as ERK1/2 signalling (Figure 2F). The differentially methylated transcripts detected in the heart failure model were also linked to metabolic processes and mitochondrial functions and especially hypermethylated transcripts were also involved in cardiac muscle development (Figure 2H).

m6A RNA methylation in the human heart

The key enzymes, METTL3, METTL4 and FTO, were expressed in the human heart (Figure 3A and online supplementary Figure S9). MeRIP-Seq analysis from non-failing hearts ($n = 5$; online supplementary Table S2) showed a substantial number of transcripts

carrying m6A marks (Figure 3B and online supplementary Table S5) and a motif search confirmed the previously described m6A RNA methylation motif (Figure 3C).

The distribution of m6A along transcripts was similar to the mouse (Figure 3D and online supplementary Figure S5). Also, in line with the mouse data, most m6A marks occurred in the CDS and 5'UTR of the corresponding transcripts (Figure 3E). A substantial number of transcripts carried m6A marks exclusively within the 3'UTR (Figure 3E). GO term analysis revealed that m6A containing transcripts encoded proteins linked to cardiomyocyte functions such as 'sarcomere organization', intracellular signalling and metabolic pathways (Figure 3F and 3G). Similar to the mouse data, we observed a mild correlation of transcript levels and m6A RNA methylation at the 5'UTR and CDS ($r = 0.19$, $P = 3.85e-08$), while no significant correlation was seen for the 3'UTR ($r = -0.05$, $P = 0.3248$) (Figure 3H). Comparison of the m6A-containing transcripts detected in the healthy mouse and human heart revealed a significant overlap of m6A-containing transcripts among the two species (representation factor 7.6, $P < 2.37e-21$; Figure 3I). It has to be mentioned that more m6A methylated transcripts were detected in mouse heart when compared to the human heart (Figures 1B and 3B). While these data likely reflect species differences, we cannot exclude that also methodological issues play a role. For example, the preparation of tissue takes 5 min in case of humans but less than 1 min in the mouse model, which correlates with RNA integrity values [RIN; 9.00 ± 0.23 for mouse and 7.80 ± 0.57 for human (mean \pm standard deviation)]. Transcripts that were m6A methylated in both mouse and humans mainly code for proteins linked to metabolic processes, and heart and circulation system development (Figure 3I).

Next, we performed MeRIP-Seq and RNA-Seq analysis of non-failing and end-stage heart failure biopsies ($n = 6$ per group; online supplementary Table S1). In line with the mouse data, we observed that – using FDR < 0.05 and two-fold change cut-off in both cases – more transcripts displayed m6A methylation changes ($n = 1246$) than genes that were differentially expressed ($n = 228$) (Figure 4A; online supplementary Figure S6A and Table S4). The differentially expressed genes were mainly linked to processes of

Figure 2 m6A RNA methylation changes associated with heart hypertrophy and heart failure. (A) Echocardiographic phenotyping 1 week after transverse aortic constriction (TAC) (anterior wall thickness: sham 0.94 mm, TAC 1.31 mm, $P = 0.0001$; ejection fraction: sham 61%, TAC 59%, $P = 0.6172$). (B) Echocardiographic phenotyping 8 week after TAC (anterior wall thickness: sham 0.983 mm, TAC 1.351 mm, $P = 0.0001$; ejection fraction: sham 59%, TAC 46%, $P = 0.0002$). Values represent mean \pm standard error of the mean ($n = 6$ animals per group except for sham 8 weeks with 5 mice available). (C) Left panel: Bar chart showing the number of genes differentially methylated and differentially expressed in the TAC model for cardiac hypertrophy. Right panel: Pie charts showing the distribution of m6A RNA methylation changes across hyper- and hypomethylated transcripts. (D) Left panel: Bar chart showing the number of differentially m6A methylated and differentially expressed genes in the TAC model for heart failure. Right panel: Pie charts showing the distribution of m6A RNA methylation changes across hyper- and hypomethylated transcripts. (E) Distribution of hyper- and hypomethylated peaks along the gene body in the TAC model for cardiac hypertrophy. (F) Gene ontology analysis (left panel) and integrated genome browser views of representative transcripts (right panel) hypo- and hypermethylated in cardiac hypertrophy. (G) Distribution of hyper- and hypomethylated peaks along the gene body in heart failure. Significant enrichment of hypomethylation at 5'UTR was observed [hypomethylation: area under the curve (AUC) = 0.2733, 95% confidence interval (CI) 0.2731–0.2735; hypermethylation: AUC = 0.1617, 95% (CI) 0.1614–0.1619]. (H) Gene ontology analysis (left panel) and integrated genome browser views of representative transcripts (right panel) hypo- and hypermethylated in the TAC model for heart failure.

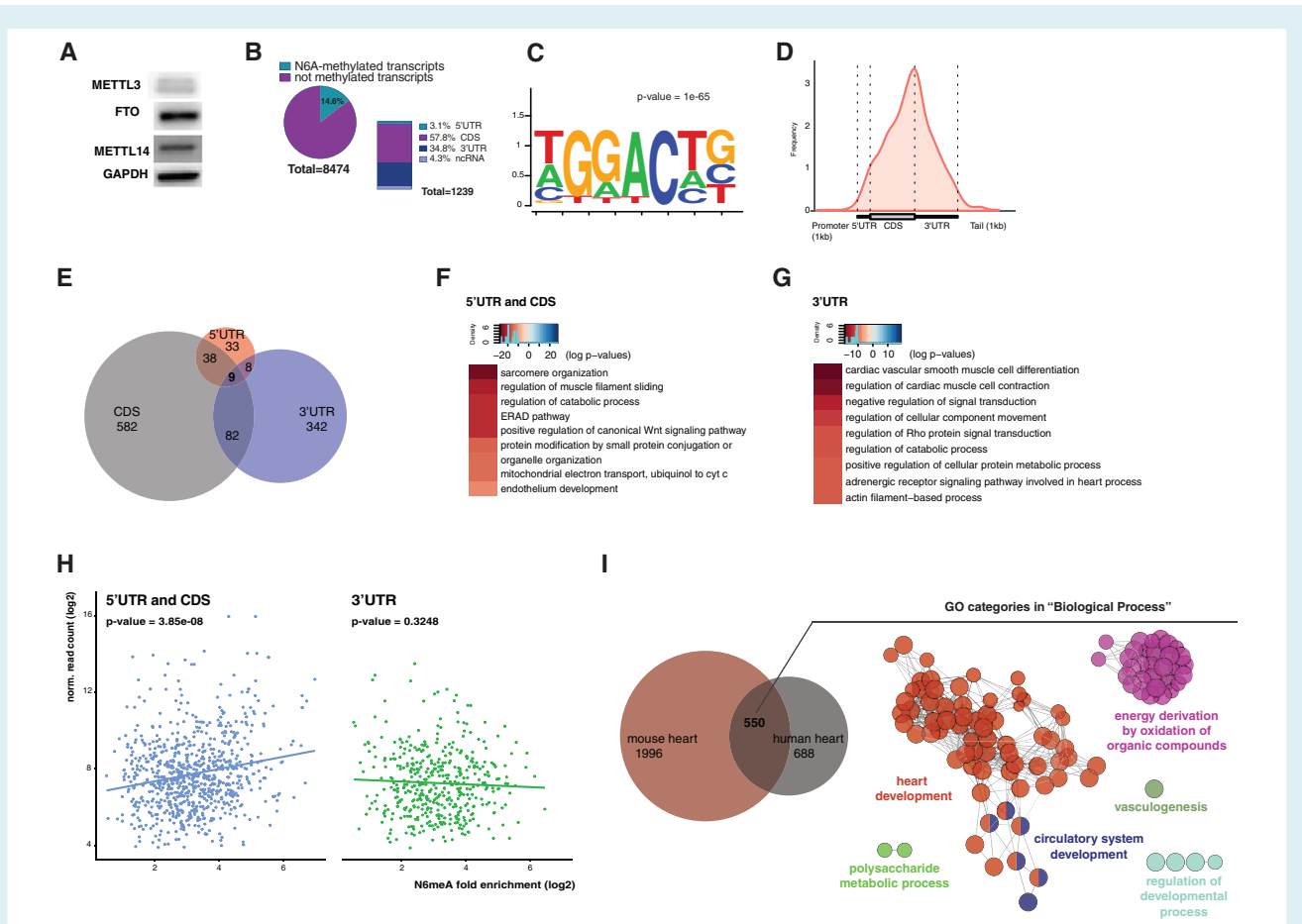


Figure 3 m6A RNA methylation in the healthy human heart. (A) Representative western blot images showing expression of FTO, METTL3 and METTL14. (B) Pie and bar charts showing the amount and distribution of m6A RNA methylation in the human heart. (C) Sequence motif identified within m6A peaks. (D) Distribution of m6A peaks across mRNA transcripts. (E) Venn diagram showing m6A marks across transcript regions. (F) Heat map showing pathway analysis of transcripts that carry m6A methylation marks in 5'UTR and CDS. (G) Heat map showing pathway analysis of transcripts that carry m6A methylation marks in 3'UTR. (H) Correlation analysis between transcript level and m6A methylation at 5'UTR and CDS (left panel) and 3'UTR (right panel). (I) Left panel: Venn diagram depicting a significant overlap (representation factor 7.6, $P < 2.37 \times 10^{-21}$) of genes encoding methylated transcripts in cardiac tissue of mice and humans. Right panel: Gene ontology categories for transcripts commonly observed in the mouse and human heart.

structural plasticity such as 'regulation of smooth cell proliferation', 'extracellular matrix organization' as well as 'metabolic function' (online supplementary Figure S6A). Similar to our findings in mice after 8 weeks of TAC (online supplementary Figure S3B), in human failing heart tissue, genes differentially expressed were substantially different from the transcripts that underwent differential m6A methylation (online supplementary Figure S6B and Table S5) providing further evidence that changes in m6A methylation and transcript level represent different cellular responses to cardiac stress.

We found that hypermethylated transcripts were mainly linked to processes that control the 'response to muscle stretch', 'response to growth factor' as well as 'heart morphogenesis' and metabolic processes (Figure 4B). Hypomethylated transcripts were associated with 'adrenergic receptor signalling in the heart', 'negative regulation of signal transduction', mitochondrial function

and metabolic processes (Figure 4C). Comparison of differentially m6A methylated transcripts detected in mouse and human heart failure showed a significant overlap (403 transcripts, representation factor 7.8, $P < 3.851 \times 10^{-251}$) (Figure 4D). These transcripts code for proteins that are, for example, linked to 'cardiac muscle differentiation' and metabolic processes (Figure 4D). Future research is needed to analyse more heart biopsy material from patients. It will be interesting to see if the degree of m6A RNA methylation changes might be correlated to the severity of clinical parameters.

Differential m6A methylation during heart failure is linked to transcripts with altered polysome binding

The data obtained from the mouse model of heart failure and failed human heart samples suggest that changes in m6A mRNA

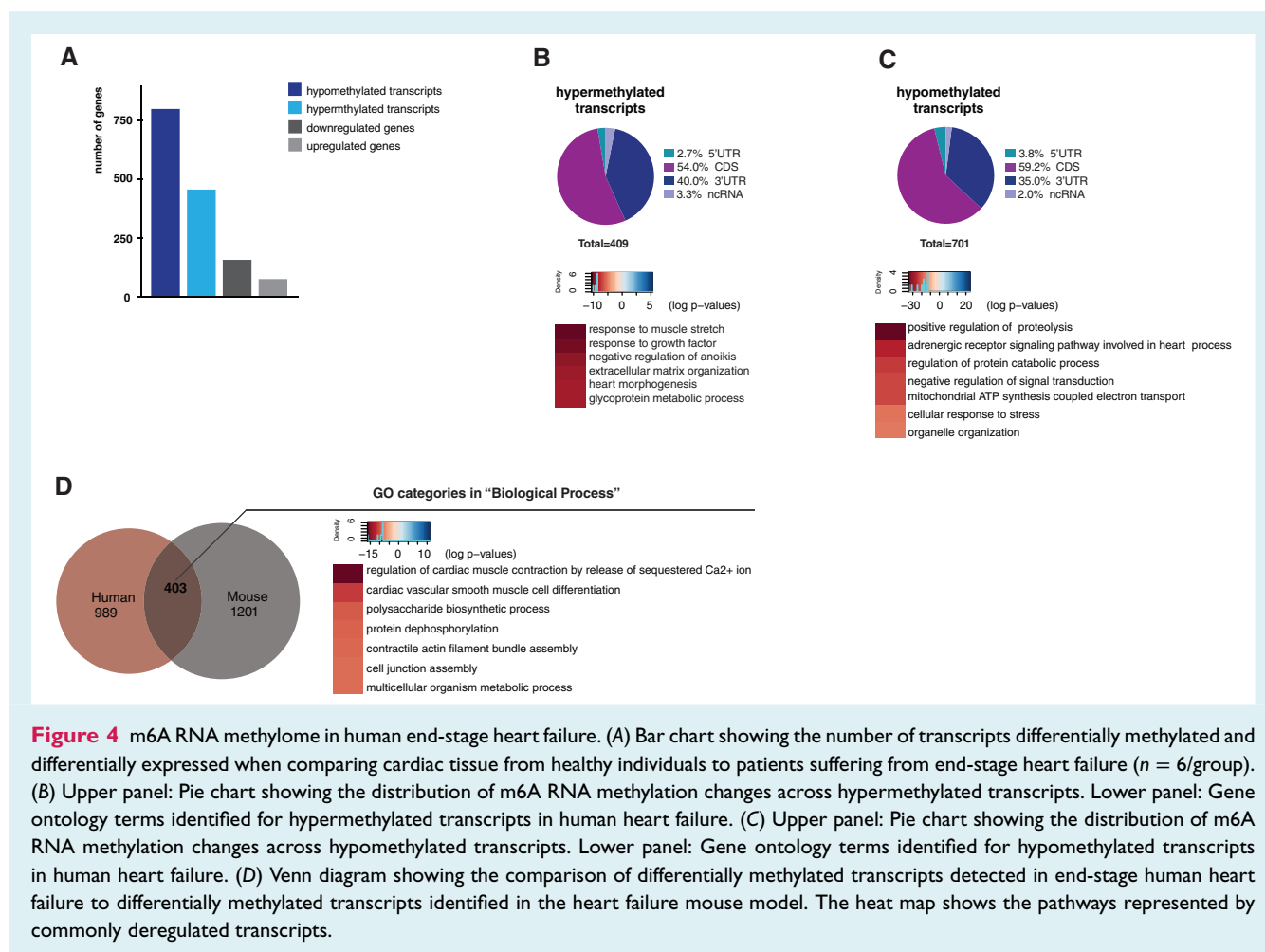


Figure 4 m6A RNA methylome in human end-stage heart failure. (A) Bar chart showing the number of transcripts differentially methylated and differentially expressed when comparing cardiac tissue from healthy individuals to patients suffering from end-stage heart failure ($n = 6/\text{group}$). (B) Upper panel: Pie chart showing the distribution of m6A RNA methylation changes across hypermethylated transcripts. Lower panel: Gene ontology terms identified for hypermethylated transcripts in human heart failure. (C) Upper panel: Pie chart showing the distribution of m6A RNA methylation changes across hypomethylated transcripts. Lower panel: Gene ontology terms identified for hypomethylated transcripts in human heart failure. (D) Venn diagram showing the comparison of differentially methylated transcripts detected in end-stage human heart failure to differentially methylated transcripts identified in the heart failure mouse model. The heat map shows the pathways represented by commonly deregulated transcripts.

methylation might play a role in cardiac function. Generally, RNA methylation has been associated with an altered mRNA decay rate,^{20,21} suggesting that changes in m6A RNA methylation may affect transcript levels. However, altered transcript levels are unlikely to be the major cellular consequence of altered m6A RNA methylation in the failing heart given that the vast majority of transcripts that exhibited changes in m6A levels were not differentially expressed (online supplementary Figures S3A,B and S4). In line with these data, the correlation of differentially methylated transcripts with their expression levels in mice and humans was not different to genes at baseline expression (online supplementary Figure S3C). Previous studies have also suggested that RNA methylation could impact mRNA translation by affecting ribosome occupancy.^{22,23} To analyse this further, we performed polysome profiling to compare transcripts bound to translating ribosomes²⁴ in mouse heart tissue 8 weeks post-sham/TAC.

We identified 225 transcripts that were significantly enriched or depleted from polysome fractions 8 weeks after TAC (Figure 5A and online supplementary Table S4). Transcripts depleted from polysomes were almost exclusively linked to metabolic processes, while those that were enriched mRNAs were involved in pathways such as calcium signalling, smooth muscle-related processes

and apoptosis (Figure 5A). Differentially methylated and differentially polysome-bound transcripts 8 weeks after TAC showed a significant positive correlation of ($r = 0.37$, $P < 2.2 \times 10^{-16}$; Figure 5B), indicating an effect of m6A methylation on polysome binding. Interestingly, this correlation was specific to transcripts that underwent differential m6A methylation after TAC, since no such correlation was observed in the sham control group (online supplementary Figure S4).

In order to provide first evidence that altered polysome binding could be a mechanism by which m6A RNA methylation impacts on cardiac plasticity in the human heart as well, we compared the 403 transcripts that exhibited altered m6A methylation in both mouse and human heart failure (Figure 4D) with our mouse polysome-bound transcripts and found a significant positive correlation (Figure 5C). Enrichment analyses of these transcripts showed pathways essential for cardiac function and metabolic processes (Figure 5D). Furthermore, we verified differential m6A RNA methylation by qRT-PCR analysis for *Calm1* and some other mRNAs by analysing input and m6A immunoprecipitated RNA samples from heart tissue of mice after 8 weeks of TAC surgery with qRT-PCR (Figure 5E and online supplementary Figure S8). mRNAs of the selected candidate genes showed no change in RNA expression while their methylation levels differed in the failing heart. Western

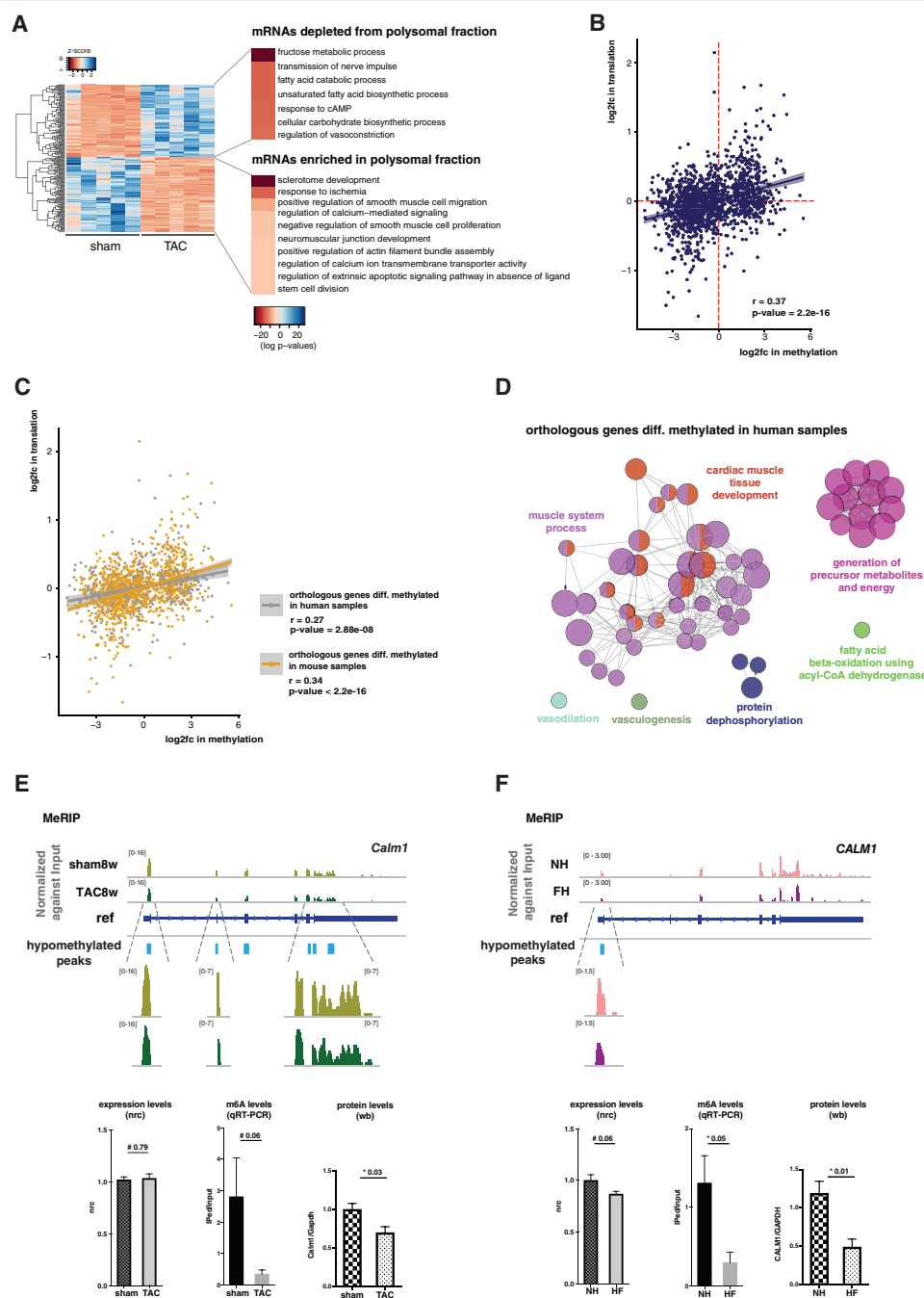


Figure 5 Changes in m6A RNA methylation during heart failure correlate with changes in polysome occupancy. (A) Heat map showing transcripts with significantly altered polysome association in the heart failure mouse model ($n = 5$ per group, $\text{Padj} < 0.05$, cut-off of fold change was set at >2.0 for enriched mRNAs and <0.5 for depleted mRNAs) and the corresponding gene ontology categories (B). Comparison of transcripts exhibiting altered m6A methylation in the heart failure mouse model with polysome occupancy reveals a significant correlation ($r = 0.37$, $P = 2.2 \times 10^{-16}$). (C) Human orthologous genes show significant correlation when calculated separately ($r = 0.27$, $P = 2.88 \times 10^{-8}$). (D) Gene ontology categories for genes showing differential methylation in human failing heart tissue and differential binding to polysomes in the mouse model of heart failure. (E) Verification of methylation changes for *Calm1* transcript in the mouse model for failed heart [8 weeks after transverse aortic constriction (TAC)]. MeRIP analysis showed hypomethylation, which was confirmed by qRT-PCR analysis of m6A precipitated RNA ($n = 4$ per group, mean \pm standard errors are shown). Transcript levels of murine *Calm1* is not changed, while western blot analysis revealed significantly reduced amount of Calm1 protein. (F) Hypomethylation of *CALM1* transcript identified by MeRIP was confirmed with qRT-PCR approach in failed human heart tissue. While transcript levels showed a trend toward downregulation in impaired heart, corresponding protein levels decrease significantly ($n = 3$ per group, mean \pm standard errors are shown).

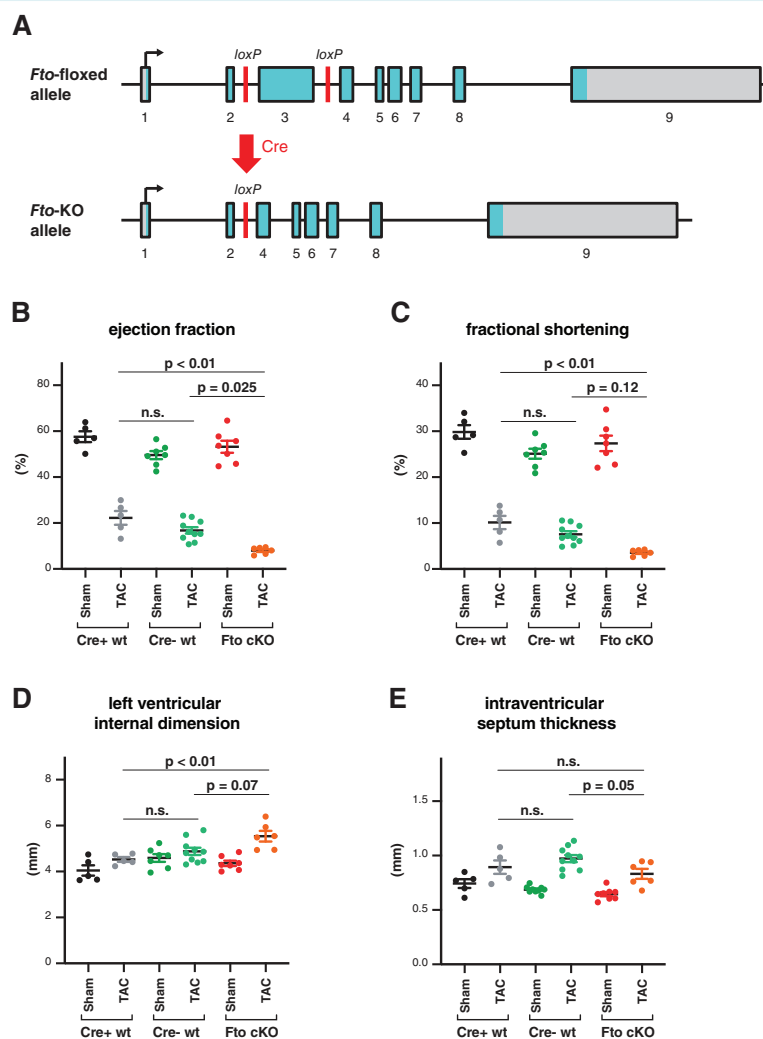


Figure 6 Fto-knockout mice show a worsened cardiac phenotype after transverse aortic constriction (TAC) surgery. (A) Scheme of generation Fto KO mice. Introns are 10× reduced while exon 2 and exon 3 are slightly enlarged for better visualization. Mice without Fto in cardiomyocytes showed significantly reduced ejection fraction (B) and fractional shortening (C), while degree of dilatation increases (D,E). $n = 5$ for Cre+ wild-type animals, $n = 7$ for Cre- wild-type and Fto-KO mice. Mean values with standard errors are depicted.

blot analysis of Calm1 and Smyd1 proteins revealed decrease levels as well (Figure 5E and online supplementary Figure S8). The same results gave analysis of human heart samples – mRNA levels of CALM1 was not affected in failed heart tissue while hypomethylation revealed by MeRIP was confirmed with qRT-PCR and the protein level decreased significantly (Figure 5F). In summary, these data suggest that altered m6A methylation of mRNA affects polysome binding of the corresponding transcripts in the heart and thus has an impact on proteostasis in a transcription-independent manner.

Fto-knockout mice show a worsened cardiac phenotype

To provide further evidence that m6A levels play a role in normal cardiac function, we generated mice that lack m6A demethylase Fto

in cardiomyocytes (Fto-KO) (Figure 6A and online supplementary Figure S10). Compared to Cre- wild-type (wt) and Cre+ wt control mice, Fto-cKO mice showed a more severe reduction in ejection fraction (16.2% and 22.25% vs. 8.01%, Cre- wt and Cre+ wt vs. Fto-cKO, respectively) and a higher degree of dilatation upon TAC surgery (4.85 and 4.52 mm vs. 5.54 mm, Cre- wt and Cre+ wt vs. Fto-cKO, respectively) (Figure 6B–E). Thus, cardiac function depends on the presence of the Fto demethylase and the cellular m6A landscape.

Discussion

Our study reveals that (i) m6A RNA methylation is altered in heart hypertrophy and heart failure; (ii) m6A RNA methylation degree positively correlates with ribosomal occupancy, leading to

increased and decreased protein levels for hyper- and hypomethylated transcripts, respectively; (iii) m6A RNA methylation levels affect protein abundance of genes that do not change their mRNA levels, pointing to the transcription-independent mechanism of translation regulation; (iv) modulation of the m6A RNA system by cardiomyocyte specific knockout of the demethylase Fto leads to a faster progression of heart failure with significant reduction in ejection fraction and increased dilatation.

Changes in transcriptome and epitranscriptome in heart failure

When we investigated m6A RNA methylation during heart failure development, we found that the number of RNAs with altered methylation levels was much higher than the number of genes that change their mRNA levels, meaning that changes in m6A RNA methylation exceed changes in gene expression. It is important to note that we applied the same cut-off to determine significant changes in either gene expression or m6A RNA methylation, thereby allowing a direct comparison. Interestingly, changes in m6A RNA methylation mainly occur in transcripts coding for proteins involved in cardiac signalling and metabolic processes whereas changes in gene expression were mainly linked to structural targets. Therefore, m6A RNA methylation is likely to influence the very early steps of gene expression regulation since transcripts encoding several transcription factors (FOXO1, FOXO4, ELF2, EIF5a), epigenetic proteins (SMYD1, DICER1, RBM20) and corresponding regulators of signalling pathways up-stream of gene expression (for example ERK and MDM2) are differentially methylated. Small changes in the expression of these 'regulatory' targets might lead to more profound changes of their downstream targets and therefore m6A RNA methylation could have a larger impact on the cardiac phenotype.

Transcription-independent effect of m6A RNA methylation

As m6A RNA methylation is present and furthermore changes also in transcripts that do not change their mRNA levels, m6A RNA methylation could affect mRNA translation and hence the proteome independent of transcription. For example, we could show, that the protein abundance of calmodulin 1 (Calm1) – a member of the important CaMKII signalling pathway – is reduced while its mRNA level is unaffected but m6A RNA methylation decreases. This shows that until now, the focus on RNA expression regulation is insufficient to describe the changes in protein abundance and that additional mechanisms – like m6A RNA methylation – can contribute to changes in the levels of proteins and, in our case, to heart failure development. This could also help to explain the often observed discrepancy between disease-associated changes in mRNA levels and the corresponding protein level.^{25,26}

Biological importance of m6A RNA methylation

We reasoned that m6A marks on different regions of transcripts might have diverse influence on mRNA, like RNA stability,

transport, ribosomal binding and decay. To our knowledge this is one of the first studies showing a link between transcript levels and the extent of m6A methylation at 5'UTR and CDS but not 3'UTR and non-coding RNAs. m6A RNA methylation was described to play a role in promoting mRNA decay.²¹ The correlation of m6A RNA methylation and transcript levels in cardiac tissue is however comparatively small, suggesting that m6A RNA methylation in the heart does not have a major effect on RNA decay. Indeed, studies in other tissues reported that m6A RNA methylation also affects processes such as translation initiation and/or efficiency.^{22,23} Since we found a correlation between m6A RNA methylation and ribosomal occupancy, we believe that this mechanism is present in the heart. Also m6A RNA methylation can affect other RNA-based processes, for example RNA transport.^{14,27,28} These different consequences of m6A RNA methylation are most likely mediated by specific m6A RNA methylation reader proteins^{10,20} but the details of such a regulation are currently not well understood. More research is needed to increase the understanding of the functions of m6A methylation in the heart and the mechanisms by which these effects are exerted.

Mechanisms underlying m6A RNA methylation changes

Our study, showing differential m6A methylation in cardiac tissue in case of heart failure, is in agreement with recent reports.^{15,29,30} Mathiyalagan *et al.*¹⁵ showed that m6A methylation is involved in the regeneration of the infarct/peri-infarction area, whereas Dorn *et al.*²⁹ and Kmietczyk *et al.*³⁰ reported that the hypertrophic response is altered in Mettl3-knockout mice leading to heart failure after TAC. This is interesting since our study shows that also Fto-cKO leads to a faster progression of heart failure with reduced hypertrophy. Therefore, deletion of the RNA methyltransferase (Mettl3) as well as the RNA demethylase (Fto) may impair the response to pressure overload. These data are in line with our observation that hyper- and hypomethylated transcripts are detected in response to heart insufficiency and suggest that the regulatory function of m6A RNA methylation is complex. We speculate that disturbance in either direction is linked to compromised cardiac function. It will be interesting to study to what extent other factors, including genetic predisposition, influence the direction and degree of m6A RNA methylation changes in cardiac diseases, thereby offering the possibility for stratified therapies. Moreover, since it has been shown that m6A methylation can have a stimulatory²³ or an inhibitory effect³¹ on translation, probably the location of the methylation mark within a transcript might determine the functional consequences. Further research is needed to study these possibilities.

One approach would be to elucidate the mechanisms that lead to altered m6A RNA methylation in cardiac diseases. We did not observe any changes of mRNA or protein levels of the key regulators of m6A RNA methylation (online supplementary Figure S7). The only exemption was a decrease of METTL3 protein in human tissue from heart failure patients, suggesting that the manipulation of Mettl3 and its counterplay Fto in a cell-specific and temporally-controlled manner in mice and in human-induced

pluripotent stem cell-derived cardiomyocytes might be a suitable approach for further studies. However, these regulators of m6A RNA methylation are also regulated via post-translational modifications^{13,32} and in case of FTO, shuttling between nucleus and cytoplasm has been reported.³³ Whether any of these processes could explain the changes in m6A RNA methylation alteration during heart failure development remains to be investigated.

In conclusion, our data shows that m6A RNA methylation is deregulated during heart failure progression. m6A RNA methylation changes are linked to changes in protein translation, even for genes that do not change their mRNA levels. This uncovers a new mechanism of translation regulation, independent of transcription. Therefore, our data suggest that modulation of epitranscriptomic processes, such as m6A RNA methylation, might be an interesting target for therapeutic interventions.

Clinical perspective

Here we could show that methylation of RNA is changed in cardiac hypertrophy and heart failure. We suggest a novel mechanism where RNA methylation influences RNA–ribosome interaction and leads to a change in protein expression and heart failure progression. Importantly, this is also true for targets that show no change in RNA expression level. This shows that protein expression regulation in heart failure occurs partially only on the translational level and without changes in DNA to RNA transcription. Therefore, this novel mechanism opens potential new treatment options for heart failure.

Supplementary Information

Additional supporting information may be found online in the Supporting Information section at the end of the article.

Methods S1. Supplementary methods.

Figure S1. m6A landscape of non-coding RNA. (A) 1.15% of all detected m6A peaks in normal heart tissue of mouse ($n = 3208$) were mapped to non-coding RNA ($n = 37$). (B) Correlation analysis between the methylation levels of non-coding RNA and transcript abundance of the same molecules. In contrast to the finding for 5'UTR and coding sequence, no relationship was revealed for non-coding RNAs between these two values ($r = 0.06$, $P = 0.7188$).

Figure S2. Gene expression changes in hypertrophic and failing heart of mouse. (A) RNA-Seq followed by differential gene expression revealed 73 genes upregulated and 83 genes downregulated after 1 week of TAC surgery ($\text{Log2FC} > 1$, $\text{Padj} < 0.05$). Lower part shows GO categories identified for deregulated genes. (B) Eight weeks after TAC surgery, 144 genes showed increased levels of transcripts while 91 genes were detected with reduced transcript abundance. Pathway analysis of differentially expressed genes showed that both metabolic and cardiac function are affected. (C) Venn diagram showing that 71 genes were differentially expressed

1 week and 8 weeks after TAC surgery. Gene enrichment analysis indicated that those genes participate in important cardiac pathways.

Figure S3. Differentially methylated transcripts outnumber differentially expressed RNAs. (A) One week after TAC surgery 217 genes showed deregulation at the transcript levels while RNAs generated from 1611 loci were detected as differentially methylated. Only 78 genes encoded transcripts differentially expressed and differentially methylated at the same time ($\text{Log2FC} > 1$, $\text{Padj} < 0.05$ cut-offs were used for both, differential expression and differential methylation analysis). (B) Left panel: 47 genes showed differential methylation and differential expression 8 weeks after surgery compared to their control group. Many more genes with differentially methylated RNAs ($n = 1182$) than differentially expressed ($n = 174$) were detected. Right panel: Venn diagram of differentially methylated, differentially transcribed and differentially translated genes in the heart failure model. (C) Correlation analysis between the levels of methylation and abundance of transcripts that changed their methylation degrees in failed heart tissue in mouse (left panel) and human (right panel).

Figure S4. Analysis of correlation between the levels of methylation and polysome occupancy in healthy heart tissue of mouse. No correlation ($r = 0.003$, $P = 0.8765$) was revealed between the levels of RNA N6A methylation and polysome binding for those RNAs in control group of mouse.

Figure S5. Epitranscriptome of human heart tissue. (A) Distribution of m6A peaks across lncRNA. (B) No correlation was found between the levels of methylation and abundance for non-coding RNAs ($r = -0.09$, $P = 0.6895$). (C) Guitar plots showing distribution of peaks with gained and lost methylation levels in human patients with heart failure.

Figure S6. Changes in transcriptome of heart tissue in human patients. (A) Differential gene expression analysis revealed 228 genes with altered transcript levels ($\text{Log2FC} > 1$, $\text{Padj} < 0.05$). mRNAs from only 30 loci were differentially methylated at the same time (B). As shown in the mouse model of heart failure, in human patients in compromised heart tissue much more transcripts show differential methylation ($n = 1249$) than differential expression ($n = 228$). Pathway analysis of differentially expressed genes revealed importance of those proteins in organization of actomyosin structure, response to stress and formation of extracellular matrix.

Figure S7. Expression of members of m6A machinery. (A) RNA-Seq data did not reveal differential expression of m6A writers, readers and erasers in mouse model of heart hypertrophy (A) and heart failure (B). No changes were detected on the level of proteins for Fto, Mettl14 and Mettl16 genes while Mettl3 showed mild reduction of protein levels in mouse failing heart samples. (C) RNA expression analysis of different genes related to m6A in human failing heart samples. Western blot analysis of METTL3, METTL14 and FTO protein showed no difference in abundance between healthy and failed human heart tissue.

Figure S8. Verification of differential m6A methylation by qRT-PCR. *Smyd1*, *Gata6* and *Rnd3* transcripts were selected

to verify MeRIP data by qRT-PCR of m6A immunoprecipitated samples from heart RNA obtained from the new batch of animals 8 weeks after TAC surgery ($n = 4$ per group). mRNAs from *Smyd1* and *Gata6* showed hypomethylation, while for *Rnd3* mRNAs hypermethylation was confirmed by showing increased trend of ratio of IPed/input in TAC mice compared to sham animals. Western blot analysis of *Smyd1* protein revealed reduction.

Figure S9. Western blot analysis of m6A RNA machinery. Full western blots are provided for main members of RNA methyltransferase and RNA demethylase for both mouse and human heart tissues.

Figure S10. Generation of Fto-cKO mice. A machinery. (A) qRT-PCR analysis shows reduction of Fto mRNA by 80% in heart tissue of Fto-cKO mice. (B) Western blot analysis revealed depletion of Fto protein from isolated cardiomyocytes of Fto-cKO animals, whereas in protein extract from the whole left ventricle contains some detectable Fto protein.

Table S1. Patient characteristics and received treatments.

Table S2. Parameters of healthy human donors.

Table S3. m6A RNA methylation in mouse heart hypertrophy. Lists of differentially methylated and differentially expressed genes are provided

Table S4. m6A RNA methylation in mouse heart failure. Lists of differentially methylated and differentially expressed genes are provided. Transcripts showing differential polysome binding are listed

Table S5. m6A RNA methylation in human heart failure. Lists of differentially methylated and differentially expressed genes are provided

Acknowledgements

We gratefully acknowledge the excellent technical assistance of S. Koszewa, A. Kretschmar, S. Zaffar, B. Knocke, R. Blume, and M. Zoremba. Great thanks to Chantal and Ferdinand for making this project possible. AF, GH were supported by the DFG under Germany's Excellence Strategy – EXC 2067/1 390729940.

Funding

This work was supported by the German Research Foundation (DFG, SFB1002 project D04 to A.F. & K.T., D01 to G.H. and BO3442/2-2 in SPP1784 to M.T.B.). The work was furthermore supported by the following funds to A.F.: DFG project FI179, the DFG priority program 1738 (FI981), an ERC consolidator grant DEPICODE (648898), the BMBF projects ENERGI (01GQ1421A) and Intergrament (01ZX1314D), and funds from the German Center for Neurodegenerative Diseases (DZNE) and German Center for cardiovascular research (DZHK).

Conflict of interest: none declared.

References

- Savarese G, Lund LH. Global public health burden of heart failure. *Card Fail Rev* 2017;3:7–11.
- Azevedo PS, Polegato BF, Minicucci MF, Paiva SAR, Zornoff LAM. Cardiac remodeling: concepts, clinical impact, pathophysiological mechanisms and pharmacologic treatment. *Arq Bras Cardiol* 2016;106:62–69.
- Toischer K, Rokita AG, Unsöld B, Zhu W, Kararigas G, Sossalla S, Reuter SP, Becker A, Teucher N, Seidler T, Grebe C, Preuss L, Gupta SN, Schmidt K, Lehnart SE, Krüger M, Linke WA, Backs J, Regitz-Zagrosek V, Schäfer K, Field LJ, Maier LS, Hasenfuss G. Differential cardiac remodeling in preload versus afterload. *Circulation* 2010;122:993–1003.
- Chatterjee K. Pathophysiology of systolic and diastolic heart failure. *Med Clin North Am* 2012;96:891–899.
- Anand P, Brown JD, Lin CY, Qi J, Zhang R, Artero PC, Alaiti MA, Bullard J, Alazem K, Margulies KB, Cappola TP, Lemieux M, Plutzky J, Bradner JE, Haldar SM. BET bromodomains mediate transcriptional pause release in heart failure. *Cell* 2013;154:569–582.
- Steenman M, Chen Y-W, Le Cunff M, Lamirault G, Varró A, Hoffman E, Léger JJ. Transcriptomal analysis of failing and nonfailing human hearts. *Physiol Genomics* 2003;12:97–112.
- Gilsbach R, Schwaderer M, Preissl S, Grüning BA, Kranzhöfer D, Schneider P, Nührenberg TG, Mulero-Navarro S, Weichenhan D, Braun C, Dreßen M, Jacobs AR, Lahm H, Doenst T, Backofen R, Krane M, Gelb BD, Hein L. Distinct epigenetic programs regulate cardiac myocyte development and disease in the human heart in vivo. *Nat Commun* 2018;9:391.
- Fu Y, Dominissini D, Rechavi G, He C. Gene expression regulation mediated through reversible m6A RNA methylation. *Nat Rev Genet* 2014;15:293–306.
- Roundtree IA, Evans ME, Pan T, He C. Dynamic RNA modifications in gene expression regulation. *Cell* 2017;169:1187–1200.
- Yang Y, Hsu PJ, Chen YS, Yang YG. Dynamic transcriptomic m6A decoration: writers, erasers, readers and functions in RNA metabolism. *Cell Res* 2018;28:616–624.
- Warda AS, Kretschmer J, Hackert P, Lenz C, Urlaub H, Höbartner C, Sloan KE, Bohnsack MT. Human METTL16 is a N6-methyladenosine (m6A) methyltransferase that targets pre-mRNAs and various non-coding RNAs. *EMBO Rep* 2017;18:2004–2014.
- Yue Y, Liu J, He C. RNA N6-methyladenosine methylation in post-transcriptional gene expression regulation. *Genes Dev* 2015;29:1343–1355.
- Yeo GS, O'Rahilly S. Uncovering the biology of FTO. *Mol Metab* 2012;1:32–36.
- Zheng G, Dahl JA, Niu Y, Fedorcsak P, Huang CM, Li CJ, Vågbo CB, Shi Y, Wang WL, Song SH, Lu Z, Bosmans RP, Dai Q, Hao YJ, Yang X, Zhao WM, Tong WM, Wang XJ, Bogdan F, Furu K, Fu Y, Jia G, Zhao X, Liu J, Krokan HE, Klungland A, Yang YG, He C. ALKBH5 is a mammalian RNA demethylase that impacts RNA metabolism and mouse fertility. *Mol Cell* 2013;49:18–29.
- Mathiyalagan P, Adamiak M, Mayourian J, Sassi Y, Liang Y, Agarwal N, Jha D, Zhang S, Kohlbrenner E, Chepurko E, Chen J, Trivieri MG, Singh R, Bouchareb R, Fish K, Ishikawa K, Lebeche D, Hajjar RJ, Sahoo S. FTO-dependent N6-methyladenosine regulates cardiac function during remodeling and repair. *Circulation* 2019;139:518–532.
- Cui X, Meng J, Zhang S, Chen Y, Huang Y. A novel algorithm for calling mRNA m6A peaks by modeling biological variances in MeRIP-seq data. *Bioinformatics* 2016;32:i378–i385.
- Dominissini D, Moshitch-Moshkovitz S, Schwartz S, Salmon-Divon M, Ungar L, Osenberg S, Cesarkas K, Jacob-Hirsch J, Amariglio N, Kupiec M, Sorek R, Rechavi G. Topology of the human and mouse m6A RNA methylomes revealed by m6A-seq. *Nature* 2012;485:201–206.
- Chang M, Lv H, Zhang W, Ma C, He X, Zhao S, Zhang ZW, Zeng YX, Song S, Niu Y, Tong WM. Region-specific RNA m6A methylation represents a new layer of control in the gene regulatory network in the mouse brain. *Open Biol* 2017;7:170166.
- Meyer KD, Saletore Y, Zumbo P, Elemento O, Mason CE, Jaffrey SR. Comprehensive analysis of mRNA methylation reveals enrichment in 3'UTRs and near stop codons. *Cell* 2012;149:1635–1646.
- Shi H, Wang X, Lu Z, Zhao BS, Ma H, Hsu PJ, Liu C, He C. YTHDF3 facilitates translation and decay of N6-methyladenosine-modified RNA. *Cell Res* 2017;27:315–328.
- Wang X, Lu Z, Gomez A, Hon GC, Yue Y, Han D, Fu Y, Parisien M, Dai Q, Jia G, Ren B, Pan T, He C. N6-methyladenosine-dependent regulation of messenger RNA stability. *Nature* 2014;505:117–120.
- Bodi Z, Bottley A, Archer N, May ST, Fray RG. Yeast m6A methylated mRNAs are enriched on translating ribosomes during meiosis, and under rapamycin treatment. *PLoS One* 2015;10:e0132090.
- Meyer KD, Patil DP, Zhou J, Zinoviev A, Skabkin MA, Elemento O, Pestova TV, Qian SB, Jaffrey SR. 5'UTR m6A promotes cap-independent translation. *Cell* 2015;163:999–1010.
- Chassé H, Boulben S, Costache V, Cormier P, Morales J. Analysis of translation using polysome profiling. *Nucleic Acids Res* 2017;45:e15.
- Cenik C, Cenik ES, Byeon GW, Grubert F, Candille SI, Spacek D, Alsallakh B, Tilgner H, Araya CL, Tang H, Ricci E, Snyder MP. Integrative analysis of RNA, translation, and protein levels reveals distinct regulatory variation across humans. *Genome Res* 2015;25:1610–1621.

26. de Sousa Abreu R, Penalva LO, Marcotte EM, Vogel C. Global signatures of protein and mRNA expression levels. *Mol Biosyst* 2009;**5**:1512–1526.
27. Yang X, Yang Y, Sun BF, Chen YS, Xu JW, Lai WY, Li A, Wang X, Bhattarai DP, Xiao W, Sun HY, Zhu Q, Ma HL, Adhikari S, Sun M, Hao YJ, Zhang B, Huang CM, Huang N, Jiang GB, Zhao YL, Wang HL, Sun YP, Yang YG. 5-Methylcytosine promotes mRNA export - NSUN2 as the methyltransferase and ALYREF as an m⁵C reader. *Cell Res* 2017;**27**:606–625.
28. Roundtree IA, Luo GZ, Zhang Z, Wang X, Zhou T, Cui Y, Sha J, Huang X, Guerrero L, Xie P, He E, Shen B, He C. YTHDC1 mediates nuclear export of N6-methyladenosine methylated mRNAs. *Elife* 2017;**6**:e31311.
29. Dorn LE, Lasman L, Chen J, Xu X, Hund TJ, Medvedovic M, Hanna JH, van Berlo JH, Accornero F. The N6-methyladenosine mRNA methylase METTL3 controls cardiac homeostasis and hypertrophy. *Circulation* 2019;**139**:533–545.
30. Kmietczyk V, Riechert E, Kalinski L, Boileau E, Malovrh E, Malone B, Gorska A, Hofmann C, Varma E, Jürgensen L, Kamuf-Schenk V, Altmüller J, Tappu R, Busch M, Most P, Katus HA, Dieterich C, Völkers M. m6A-mRNA methylation regulates cardiac gene expression and cellular growth. *Life Sci Alliance* 2019;**2**:e201800233.
31. Slobodin B, Han R, Calderone V, Vrielink JA, Loayza-Puch F, Elkon R, Agami R. Transcription impacts the efficiency of mRNA translation via co-transcriptional N6-adenosine methylation. *Cell* 2017;**169**:326–337.e12.
32. Wang P, Doxtader KA, Nam Y. Structural basis for cooperative function of Mettl3 and Mettl14 methyltransferases. *Mol Cell* 2016;**63**:306–317.
33. Gulati P, Avezov E, Ma M, Antrobus R, Lehner P, O'Rahilly S, Yeo GS. Fat mass and obesity-related (FTO) shuttles between the nucleus and cytoplasm. *Biosci Rep* 2014;**34**:e00144.